Uncertainty and Global Sensitivity Analysis of Wind Turbines Power Production in Non-Ideal Conditions

Bruno M. Mazetto[1], Thiago G. Ritto[1]

[1]*Dept. of Mechanical Engineering, Federal University of Rio de Janeiro*
Av. Horacio Macedo, 2030, Bloco I, Sala 130, CEP: 21941-914, Rio de Janeiro/RJ, Brazil
bmazetto@gmail.com, tritto@mecanica.ufrj.br

Abstract. Starting from a consolidated open-source software for wind turbine simulation (OpenFAST), the effects of operation in non-ideal conditions on power production of a theoretical 5 MW wind turbine are evaluated. Capacity factor (CF) and the levelized cost of energy (LCOE) for a 500-MW wind farm considering two locations, one in the northeast of Brazil and another on the North Sea, in Europe, are evaluated. Representative parameters of non-ideal operational situations are identified and probabilistic models are proposed for the associated uncertainties. Afterward, propagation of uncertainties through Monte Carlo simulations is carried out, and finally, supported by a global sensitivity analysis based on Sobol indexes, situations that should be primarily treated are identified. The results indicate that the mean CF is up to 9% lower and mean LCOE is up to 12% lower than their reference values. Finally, the sensitivity analysis indicates that the greatest influence on generation of the wind turbines and economic feasibility of wind farms are regarded to rotor misalignment with the wind.

Keywords: global sensitivity analysis; levelized cost of energy; Stochastic power production; Wind turbine dynamics

1 Introduction

Wind power is one of the most promising renewable sources for the energy transition. Wind farms have spread out all over the world due to decreasing costs, government incentives and technology evolution. For the latter, it can be highlighted the increase in size, height and power capacity of wind turbines and the massive use of digitalization and digital twins along the whole asset life [1]. Due to capacity evolution, although specific costs decrease, deviations from ideal operations may cause greater impact in performance and asset life than those observed for smaller wind turbines. On the other hand, digital twins provide support for strategic decision making, by promoting understanding of how these deviations can affect both efficiency and health of wind turbines.

In view of this scenario, the objective of this paper is to analyze the effects of operation under non-ideal conditions on the power of wind turbines and on the levelized cost of energy for two hypothetical 500-MW wind farms, one in the Atlantic Ocean near the northeast coast of Brazil and another in the North Sea near the southeast coast of England, helping to define priorities for preventive action and quantification of risks.

2 Non-ideal operation

Wind farm net energy generation results from wind resource, wind turbine characteristics and production losses. Part of them are due to loss of turbine performance, related to sub-optimal control settings, high wind control hysteresis and wind conditions departing from power curve design [2]. The resultant non-ideal operation do not result in the immediate cessation of generation, but compromises its performance. From the studies of Luengo and Kolios [3], Márquez et al. [4], three conditions stand out: (i) yaw misalignment; (ii) rotor aerodynamic imbalance; (iii) rotor mass imbalance.

Yaw misalignment is observed when the rotor is not facing the wind direction and is mainly caused by measurement errors linked to improper installation or poor calibration of the wind vane sensor and wind flow

distortion by blade's activities, terrain complexity or wakes of neighboring wind turbines [5]. From the studies of Hojstrup [6] and Steinmetz [7], it is responsible by 1% to 2% loss of annual energy production (AEP), in average.

In turn, rotor aerodynamic imbalance is induced by offsets in pitch and twist angles among the blades, departing from their reference values. Main causes for aerodynamic imbalance are pitch system and control loop failures or errors during assembly or manufacture process [8]. Elosegui et al. [9] verified that for discrepancies of 2° in just one blade, AEP expected loss is 1%.

At last, rotor mass imbalance results from differences between blades total masses or mass distributions due to manufacturing issues, aging degradation, wear and fatigue during operation, as well as, excessive mass addition for repair and water penetration [10]. Zhao et al. [11] showed that the mass imbalance is responsible for a delay in the starting process and fluctuation in power generation.

3 Methodology

3.1 Wind turbine and wind farm

The NREL offshore 5-MW baseline wind turbine from Jonkman et al. [12] was considered. The model represents a three-bladed, upwind horizontal axis wind turbine with rotor diameter of 126 m and hub-height of 90 m above tower base. Cut-in, rated and cut-out wind speed are 3 m/s, 11.4 m/s and 25 m/s, respectively. For the economical evaluations of this study, it was considered a hypothetical offshore wind farm with an installed capacity of 500 MW, consisting of 100 x 5-MW baseline wind turbines.

3.2 Stochastic model

The inputs assumed to be random variables were the wind speed, yaw misalignment for the rotor, pitch deviation, tip twist error and total mass of each blade, as shown in Table 1.

For wind speed at hub height, Weibull distributions are fitted to reanalysis data from 2000 to 2018 for two locations: London Array Offshore Wind Farm center location (North Sea) [13] and EOL Planta Piloto de Geração Offshore (RN/Brazil) [14].

Yaw misalignment distribution is obtained by considering data from Hojstrup [6] for the static deviation and from Song et al. [15] for the dynamic component. Pitch error probabilistic model is derived from the assumptions made by Cacciola et al. [8], Elosegui et al. [9]. For the twist offsets for the blade tip, the same distribution adopted by Robertson et al. [16], Petrone et al. [17] is applied. Besides, this value declines linearly from blade tip to root, where no twist error is produced. For the blade mass deviation, results from Braam et al. [18] analysis for a set of 37 blades of wind turbines are adapted to the 5-MW NREL wind turbine blade.

Table 1. PDFs for uncertain inputs.

Input	PDF	Reference
Wind speed (m/s)	Weibull 2-par (Figure 1)	[19]
Yaw misalignment ($^\circ$)	$Normal(0^\circ, 12.81^\circ)$	[6, 15]
Pitch error ($^\circ$)	$Normal(0^\circ, 2.1493^\circ)$	[8, 9]
Twist error ($^\circ$)	$Uniform(-2^\circ, 2^\circ)$	[16, 17]
Blade mass deviation (ton)	$Normal(17.74, 0.36)$, supported on $[15.97, 19.51]$	[18]

3.3 Monte Carlo simulations

Through SALib [20], a sensitivity analysis library for python, Sobol quasi-random sequences are used to generate samples for the uncertain inputs. As mentioned by Saltelli et al. [21], these sequences outperform crude Monte Carlo sampling in the estimation of multi-dimensional integrals, since they allow a ordered and progressive filling of the space.

Model realizations were obtained using NREL OpenFAST (Fatigue, Aerodynamics, Structures and Turbulence) Code, an open source framework composed of different modules that together provide a coupled aero-hydro-servo-elastic solution for wind turbine simulation [22].

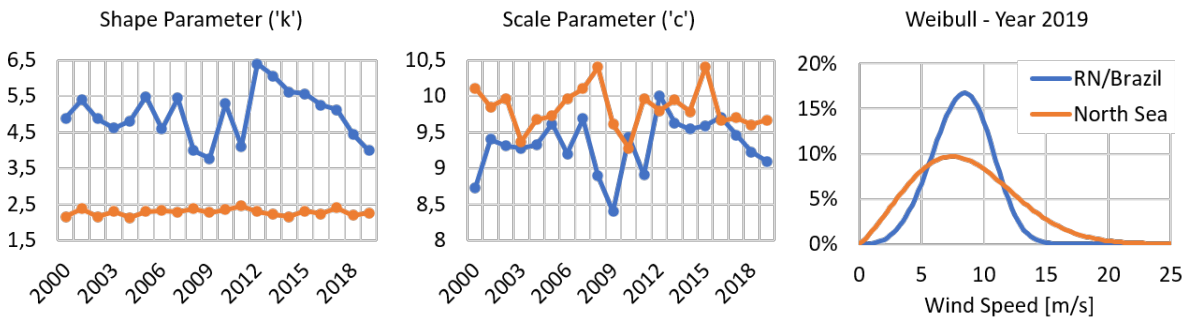

Figure 1. Weibull parameters for years 2000 to 2019 and PDF for RN/Brazil and North Sea locations in 2019.

The quantities of interest for this study are the capacity factor (CF) and levelized cost of energy (LCOE) for two hypothetical 500-MW wind farms. The first step is to get an effective power curve, considering the influence of the aforementioned uncertain inputs. To do it, 24 wind speeds are chosen between wind turbine cut-in and cut-out and, for each of them, OpenFAST is used to simulate power generation over time until steady state is reached. The mean value during this last phase is associated to the corresponding wind speed. Through linear interpolation, the effective power curve is built for the sampled set of uncertain parameters.

Once the power curve is defined, gross annual energy production (AEP) for the locations and for each year is calculated using power curve and the wind speed CDF, both discretized in n bins. Besides, a combination of losses should be considered to obtain the net AEP [2]. Equation (1) is used to get the net AEP for a wind farm, where F_i is the probability of occurrence for bin i of wind speed, P_i is power generation for bin i, T_{year} is the number of hours of the year, N_{WT} is the number of wind turbines for the wind farm and L_{tot} is the total power losses considered.

$$AEP_{net} = (1 - L_{tot})\, N_{WT} T_{year} \sum_{i=1}^{n} F_i P_i \tag{1}$$

The total loss (L_{tot}), calculated through Equation (2), is dependent on losses related to wake effects ($L_{wk} = 6.7\%$), availability ($L_{av} = 6.0\%$), electrical losses ($L_{el} = 2.1\%$), environmental ($L_{ev} = 2.6\%$) and curtailments ($L_{ct} = 0\%$) [2]. Turbine performance losses are related to the operational cases under evaluation and affect the power curve, therefore a constant factor is not applied for L_{tot} calculation.

$$L_{tot} = 1 - (1 - L_{wk})(1 - L_{av})(1 - L_{el})(1 - L_{ev})(1 - L_{ct}) \tag{2}$$

Following the net AEP, capacity factor CF is given by Equation 3, where AEP_{ideal} is the energy that would be generated if the wind farm were operated at full capacity (P_{full}) over a year (T_{year}) [23].

$$CF = \frac{AEP_{net}}{AEP_{ideal}} = \frac{AEP_{net}}{P_{full} T_{year}} \tag{3}$$

The last quantity of interest is the LCOE, which is the present value of the price of produced electrical energy considering the economic life of the plant and costs [23]. For this study, the costs considered are CAPEX (Capital Expenditures) and OPEX (Operational Expenditures), and LCOE is calculated according to Equation 4. The economical data used as input for the analysis is shown in Table 2.

$$LCOE = \frac{CAPEX + \sum_{t=1}^{T} \frac{OPEX_t}{(1+WACC)^t}}{\sum_{t=1}^{T} \frac{AEP_{net,t}}{(1+WACC)^t}} \tag{4}$$

Regarding convergence of simulations, the mean square convergence was adopted considering the quantities of interest as output parameter. It was observed that 500 simulations were enough to guarantee the convergence.

Table 2. Wind farm economical data.

Capacity (P_{full})	500 MW
Economical Life	20 years [24]
CAPEX (per MW)	4,609 USD/MW [25]
Annual OPEX (per MW)	3.5% of CAPEX [24]
Weighted Average Cost of Capital (WACC)	10% per year [24]

Moreover, for a simulated time of 60 seconds, almost 180 seconds were necessary to execute the NREL OpenFAST code, using a Intel Core i7-5500U @2.40 GHz dual core notebook with Windows 10 and 8 GB of RAM. By using parallel processing, four simulations could be carried out simultaneously, which allowed the 500 simulations per fixed wind speed to take near 6.5 hours to be concluded.

3.4 Sensitivity analysis

Sensitivity analysis is employed to understand how uncertainty in the output of a model can be apportioned to different sources of uncertainty in the model input [26]. In this study, outputs are the quantities of interest presented in 3.3 and inputs are the parameters indicated in 3.2. Moreover, a global sensitivity analysis is adopted, since it is concerned with the entire range of the input variables instead of focusing on local results.

For global sensitivity analysis, output variance is generally decomposed using ANOVA-HDMR (Analysis of Variance - High Dimensional Representation) in order to segregate the effects due to each input and also due to interactions between variables. By normalizing the decomposition terms using the total variance of the output, Sobol indexes are defined. The most useful are the first-order and the total effects indexes [26].

According to Saltelli [26], the first-order Sobol index represents the main effect of an input to the variance of the output and is employed to identify which factor, once fixed to its true value, would lead to the greatest reduction in the variance of output. First-order Sobol index (S_i) is given by Equation 5, where $V_{X_i}\left(\mathbb{E}_{\mathbf{X}_{\sim i}}(Y \mid X_i)\right)$ is the variance due to main effect of a single variable (X_i), $\mathbb{E}_{\mathbf{X}_{\sim i}}(Y \mid X_i)$ is the average of Y taken over $\mathbf{X}_{\sim i}$ (all factors but X_i), and $V(Y)$ is the variance of the output Y.

$$S_i = \frac{V_{X_i}\left(\mathbb{E}_{\mathbf{X}_{\sim i}}(Y \mid X_i)\right)}{V(Y)} \tag{5}$$

On the other hand, a total effect index account for the total contribution to the output variation due to a specific input, regarding first-order and interactions effects. Total effects indexes are used to identify factor which make no significant contribution to the output variance and, as a result, could be fixed at any given value within their range of variation. Total effects Sobol index (S_{Ti}) is given by Equation 6, where $\mathbb{E}_{\mathbf{X}_{\sim i}}\left(V_{X_i}(Y \mid \mathbf{X}_{\sim i})\right)$ is the remaining variance of Y that would be left, on average, if the true values of all variables but X_i could be determined.

$$S_{Ti} = \frac{\mathbb{E}_{\mathbf{X}_{\sim i}}\left(V_{X_i}(Y \mid \mathbf{X}_{\sim i})\right)}{V(Y)} \tag{6}$$

For calculating the indices, a python routine applying the SALib library [20] was developed. The methodology for numerically and efficiently estimate the first order and total effect indices is based on Sobol [27], Saltelli [28] and Saltelli et al. [21]. In brief, the main steps are firstly the generation of two independent matrices, where each line is formed by values drawn from the uncertain parameters distributions, followed by the definition of derived matrices related to the input and Sobol index of interest and by the computation of the model outputs for the first and derived matrices. From the results, averages and variances are estimated and used for indices calculation.

4 Results

4.1 Uncertainty Propagation

The propagation of uncertainties is firstly performed for the power curve of the 5-MW wind turbine (Figure 2). The red area represents a 95% stochastic envelope, the dashed blue line is the mean value of power production

and the dashed black line is the nominal power curve. The effects of non-idealities are more prominent for wind speeds up to 14 m/s. The gap between reference curve, mean and lower bound of the P95 envelope increases as the wind speed rises, peaking near the rated wind speed and drastically decreasing until 14 m/s, from where uncertainties produce no variation on power production.

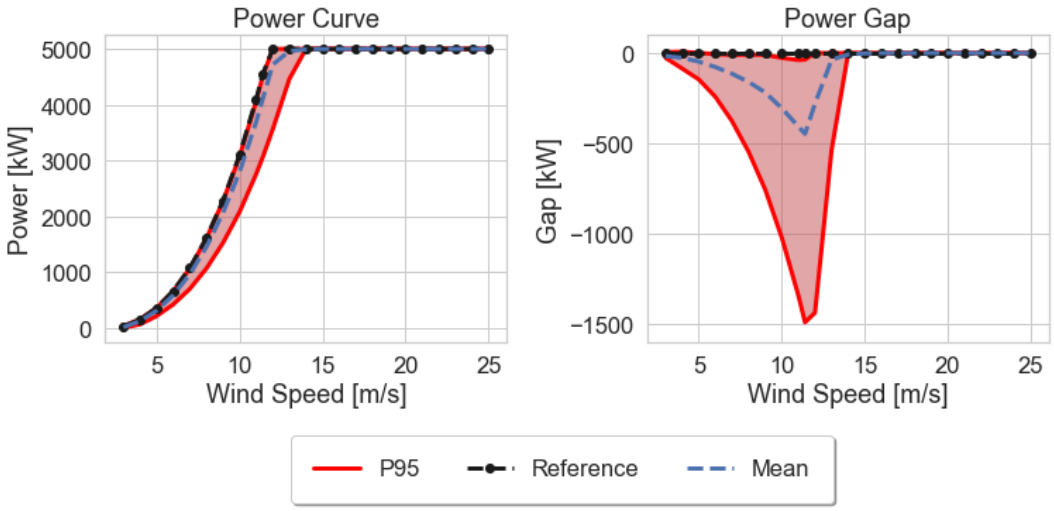

Figure 2. Uncertainty propagation for wind turbine power curve.

As consequence of uncertainties in model inputs leading to variability in power curves, CF for each wind farm along their economical life is also uncertain. Figure 3 presents the CF histogram and shows the differences observed from reference to the mean and to the lower bound of the 95% stochastic envelope.

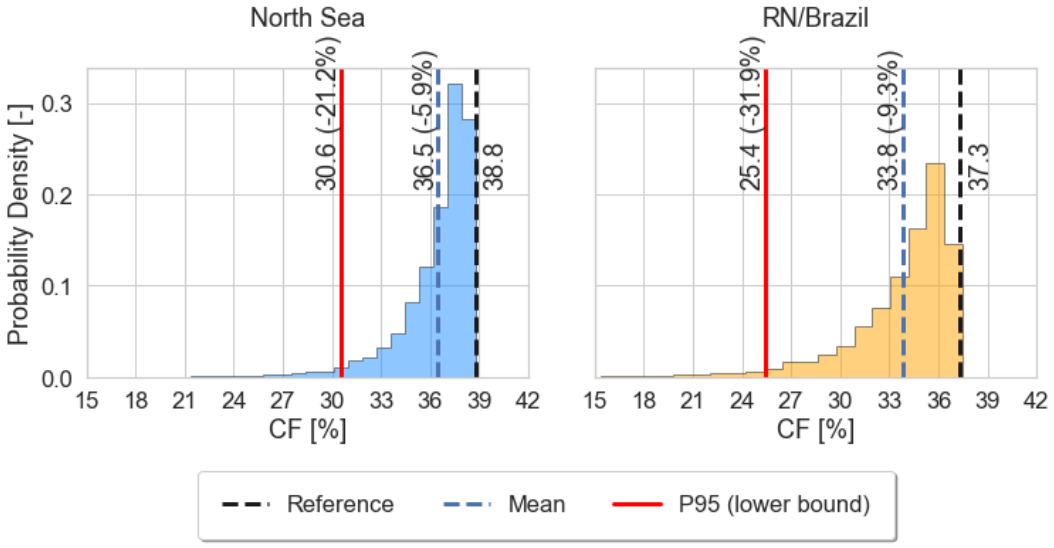

Figure 3. Capacity Factor (CF) histograms for 500-MW wind farm in the North Sea and in the Rio Grande do Norte coast (Brazil).

The histograms show similar behavior for both locations, with occurrences increasing along side CF, reaching the highest probabilities near the reference value. However, for the Brazilian wind farm, the distribution is less concentrated near the reference value than that of the North Sea. As a result, the mean and the lower bound of the envelope are also lower in absolute and relative terms.

LCOE histograms (Figure 4) show an inverted behavior to the previous ones, which is explained by LCOE dependence on the inverse of net AEP series present value. Also, input uncertainties indicate scenarios of higher LCOE, reducing economical attractiveness of the wind farms. Mean values for LCOE could be 6.7% higher for the wind farm in North Sea and 11.7% higher for Rio Grande do Norte coast than the reference value. For the extreme 2.5% resultant scenarios, LCOE could be 26.8% higher in Europe and 47% in Brazil.

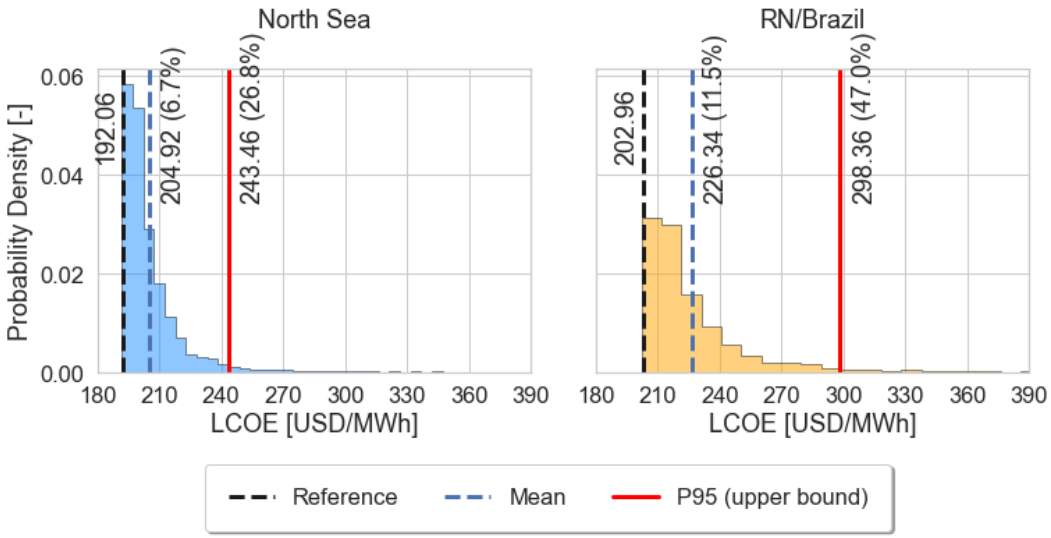

Figure 4. Levelised Cost of Energy (LCOE) histograms for 500-MW wind farm in the North Sea and in the Rio Grande do Norte coast (Brazil).

By comparing the results of uncertainty propagation on the quantities of interest, it can be verified that the same uncertain inputs cause larger effects for the Rio Grande do Norte wind farm. The main reason for this is related to the wind speed distributions. For the Brazilian location, wind speeds are basically concentrated below 15 m/s, which is the range where effects of uncertainty are also more relevant, as seen in Figure 1. On the other hand, in the European site there is a more spread distribution with relevant cumulative frequency above 15 m/s, where the effects of uncertainty on power production are negligible.

4.2 Sobol Indexes

Even though the results of uncertainty propagation are known, it is paramount to understand which inputs are the most relevant and which of them (if any) could be neglected regarding power production. By calculating first order and total effects Sobol indexes for the uncertain parameters, both goals are achieved. Figure 5 presents indexes plots for the quantities of interest and the uncertain inputs for both locations.

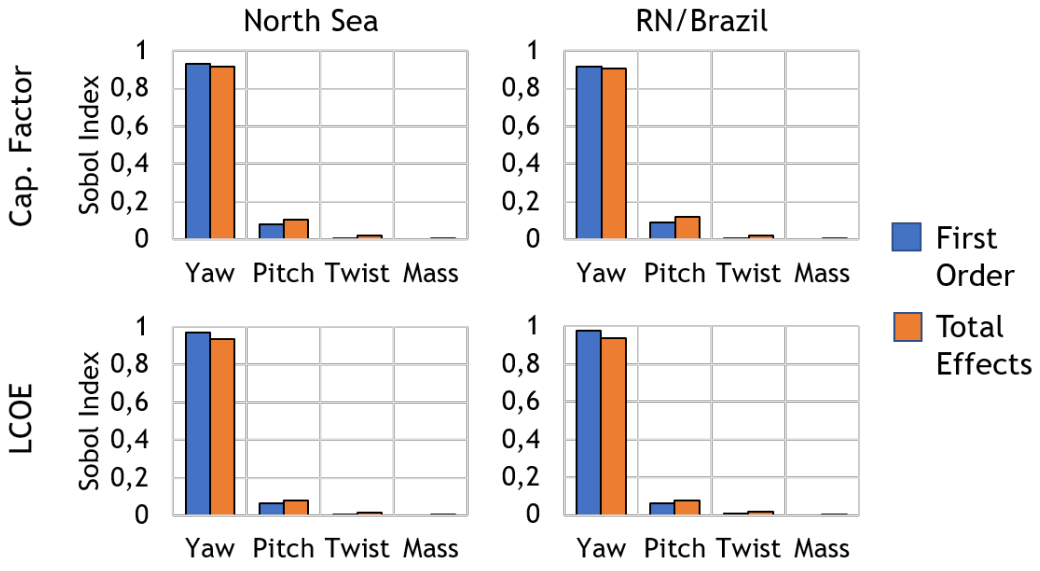

Figure 5. First order and total effects Sobol indexes.

The same pattern, independently of location and quantity of interest, is observed in all plots of Figure 5: yaw misalignment is the parameter with the highest value for first order and total effects indexes, while those for twist and mass deviations are very near to zero. Moreover, values for first order and total effects indexes for each input are close, indicating that interactions among parameters are of little relevance compared to the direct effects.

Since output variances are basically influenced by the direct effect of yaw misalignment uncertainty, whose contribution exceeds 90% in all cases, it is recommended that actions be taken to reduce yaw uncertainty. For instance, the use of nacelle-mounted LIDARs or spinner-integrated ultrasonic anemometers could minimize the uncertainty during development phase and generation loss during operation phase.

Contrarily to yaw, the influence of twist and mass deviations could be neglected for the quantities studied and could be fixed to their reference values. However, it is important to point out that these variables can still cause loss of generation and revenue, since both can increase fatigue and damage on main components, reducing their lives and causing wind turbine downtime. Another relevant consideration is that the relative importance of the uncertain inputs is dependent on the characterization of their distributions and supports. Had diverse assumptions or additional data been adopted for the stochastic modeling, other distributions would have been found for the parameters, which could have produced different results.

5 Conclusions

In this study, the influence of non-ideal operation situations on the power curve of a 5-MW reference offshore wind turbine, as well as on capacity factor and levelized cost of energy for 500-MW hypothetical wind farms on offshore sites in Europe and Brazil. To achieve the results, Monte Carlo simulations using OpenFAST code were performed and a stochastic approach was considered for the uncertain inputs. To help defining priorities for preventive action, a global sensitivity analysis using Sobol indexes was conducted.

Uncertainty propagation showed that the effective power curve for the 5-MW reference offshore wind turbine was mostly affected for wind speeds from cut-in to rated power. Considering these power curves and wind speed distributions, capacity factor would, in average, be reduced in 6% to 9% while LCOE would increase from nearly 7% to 12% for 500-MW wind farms in North Sea and RN/Brazil, respectively. The uncertainties on these outputs, as showed by sensitivity analysis, are mostly related to direct influence of yaw misalignment uncertainty and could be mitigated by the use of instruments to guarantee precise measurements during wind turbine operation.

Acknowledgements. This paper was developed as part of Petrobras "Offshore Wind Pilot Plant" project (PD-0553-0045 / 2016) within the framework of the Electric System R&D, regulated by ANEEL.

Authorship statement. The authors hereby confirm that they are the sole liable persons responsible for the authorship of this work, and that all material that has been herein included as part of the present paper is either the property (and authorship) of the authors, or has the permission of the owners to be included here.

References

[1] IRENA. Future of wind: Deployment, investment, technology, grid integration and socio-economic aspects. Technical report, International Renewable Energy Agency, Abu Dhabi, 2019.

[2] M. C. Brower. *Wind Resource Assessment: a practical guide to developing a wind project*. John Wiley & Sons, Inc., Hoboken, NJ, 2012.

[3] M. Luengo and A. Kolios. Failure mode identification and end of life scenarios of offshore wind turbines: A review. *Energies*, vol. 8, n. 8, pp. 8339–8354, 2015.

[4] F. P. G. Márquez, J. M. P. Pérez, A. P. Marugán, and M. Papaelias. Identification of critical components of wind turbines using FTA over the time. *Renewable Energy*, vol. 87, pp. 869–883, 2016.

[5] D. Choi, W. Shin, K. Ko, and W. Rhee. Static and dynamic yaw misalignments of wind turbines and machine learning based correction methods using lidar data. *IEEE Transactions on Sustainable Energy*, vol. 10, n. 2, pp. 971–982, 2019.

[6] J. Hojstrup. Increased energy production by optimization of yaw control. *VGB PowerTech*, vol. 6, pp. 62–66, 2014.

[7] G. Steinmetz. Wind analysis in operation phases: identifying and unlocking optimization capacities. In *Conférence sur l'exploitation des parcs éoliens 2016*, Paris, France, 2016.

[8] S. Cacciola, I. M. Agud, and C. Bottasso. Detection of rotor imbalance, including root cause, severity and location. *Journal of Physics: Conference Series*, vol. 753, pp. 072003, 2016.

[9] U. Elosegui, I. Egana, A. Ulazia, and G. Ibarra-Berastegi. Pitch angle misalignment correction based on benchmarking and laser scanner measurement in wind farms. *Energies*, vol. 11, n. 12, pp. 3357, 2018.
[10] H. Malik and S. Mishra. Artificial neural network and empirical mode decomposition based imbalance fault diagnosis of wind turbine using TurbSim, FAST and simulink. *IET Renewable Power Generation*, vol. 11, 2017.
[11] P. Zhao, X. Li, and L. Yang. Research on mass imbalance fault of wind turbine based on virtual prototype. *MATEC Web of Conferences*, vol. 95, pp. 06001, 2017.
[12] J. Jonkman, S. Butterfield, W. Musial, and G. Scott. *NREL/TP-500-38060: Definition of a 5-MW reference wind turbine for offshore system development*. National Renewable Energy Laboratory, Golden, 2009.
[13] 4C Offshore. London array offshore wind farm – project details. https://www.4coffshore.com/windfarms/london-array-phase-1-united-kingdom-uk14.html, 2019a.
[14] 4C Offshore. Eol planta piloto de geração offshore – project details. https://www.4coffshore.com/windfarms/paracuru-campo-eolico-brazil-br26.html, 2019b.
[15] D. Song, J. Yang, X. Fan, Y. Liu, A. Liu, G. Chen, and Y. H. Joo. Maximum power extraction for wind turbines through a novel yaw control solution using predicted wind directions. *Energy Conversion and Management*, vol. 157, pp. 587–599, 2018.
[16] A. N. Robertson, K. Shaler, L. Sethuraman, and J. Jonkman. Sensitivity analysis of the effect of wind characteristics and turbine properties on wind turbine loads. *Wind Energy Science*, vol. 4, n. 3, pp. 479–513, 2019.
[17] G. Petrone, de C. Nicola, D. Quagliarella, J. Witteveen, and G. Iaccarino. Wind turbine performance analysis under uncertainty. In *49th AIAA Aerospace Sciences Meeting*, pp. 544, 2011.
[18] H. Braam, J. Heijdra, D. v. Delft, H. v. Leeuwen, E. Jorgensen, D. Lekou, and P. Vionis. *Probability distribution of fatigue strength of rotor blades*. ECN Wind Energy, Netherlands, 2001.
[19] Lautec esox – run weather downtime simulations, 2020.
[20] J. Herman and W. Usher. SALib: An open-source python library for sensitivity analysis. *The Journal of Open Source Software*, vol. 2, n. 9, 2017.
[21] A. Saltelli, P. Annoni, I. Azzini, F. Campolongo, M. Ratto, and S. Tarantola. Variance based sensitivity analysis of model output. design and estimator for the total sensitivity index. *Computer Physics Communications*, vol. 181, n. 2, pp. 259–270, 2010.
[22] National Renewable Energy Laboratory. Openfast documentation, 2021.
[23] T. M. Letcher. *Wind Energy Engineering: A Handbook for Onshore and Offshore Wind Turbines. Chapter 1: Why Wind Energy?* Academic Press, Londres, 2017.
[24] dos M. M. L. Reis, B. M. Mazetto, and da E. C. M. Silva. Economic analysis for implantation of an offshore wind farm in the brazilian coast. *Sustainable Energy Technologies and Assessments*, vol. 43, pp. 100955, 2021.
[25] L. Array. London array: the world's largest operational offshore wind farm. *Engineering & Technology Reference*, vol. 1, 2015.
[26] A. Saltelli. *Global sensitivity analysis : the primer*. John Wiley, Chichester, England Hoboken, NJ, 2008.
[27] I. Sobol. Global sensitivity indices for nonlinear mathematical models and their monte carlo estimates. *Mathematics and Computers in Simulation*, vol. 55, n. 1-3, pp. 271–280, 2001.
[28] A. Saltelli. Making best use of model evaluations to compute sensitivity indices. *Computer Physics Communications*, vol. 145, n. 2, pp. 280–297, 2002.